Institut Pasteur
Microbes and Infection 15 (2013) 291–301
www.elsevier.com/locate/micinf

Original article

The surface proteins InlA and InlB are interdependently required for polar basolateral invasion by *Listeria monocytogenes* in a human model of the blood–cerebrospinal fluid barrier

Tim Gründler [a], Natascha Quednau [a], Carolin Stump [a], Véronique Orian-Rousseau [b], Hiroshi Ishikawa [c], Hartwig Wolburg [d], Horst Schroten [a], Tobias Tenenbaum [a], Christian Schwerk [a,*]

[a] *Pediatric Infectious Diseases, Department of Pediatrics, Medical Faculty Mannheim, Heidelberg University, Theodor-Kutzer-Ufer 1-3, D-68167 Mannheim, Germany*
[b] *Institute for Toxicology and Genetics, Karlsruhe Institute of Technology, Eggenstein-Leopoldshafen, Germany*
[c] *Department of Anatomy, Jikei University School of Medicine, 3-25-8 Nishi-Shinbashi, Minato-ku, Tokyo 105-8461, Japan*
[d] *Institute of Pathology and Neuropathology, University of Tübingen, Tübingen, Germany*

Received 30 July 2012; accepted 10 December 2012
Available online 30 January 2013

Abstract

The Gram-positive bacterium *Listeria monocytogenes* can enter the human central nervous system and cause life-threatening meningitis. During this process the pathogen has to invade and cross diverse cellular barriers involving the functions of the surface proteins Internalin (InlA) and InlB. Whereas the internalin-dependent crossing of the intestinal epithelium and the fetoplacental barrier have been subject to intensive investigation, limited research elucidating the crossing of the human blood–cerebrospinal fluid barrier (BCSFB) has been reported. We have recently established a functional *in vitro* model of the BCSFB based on human choroid plexus papilloma (HIBCPP) cells. We show polarized expression of receptors involved in listerial invasion (i.e. E-Cadherin, Met) in HIBCPP cells. Infecting HIBCPP cells with the *L. monocytogenes* strain EGD, we demonstrate polar invasion exclusively from the *in vivo* relevant basolateral cell side. Intracellular listeria were found in vacuoles and the cytoplasm, where they were often associated with "actin tail"-like structures. Furthermore, the *L. monocytogenes* wild type strain shows significantly higher internalization rates than isogenic mutants lacking either InlA, InlB or both surface proteins. Deletion of either one or both proteins leads to a similarly decreased invasion, suggesting an interdependent function of InlA and InlB during invasion of choroid plexus epithelial cells.
© 2013 Institut Pasteur. Published by Elsevier Masson SAS. All rights reserved.

Keywords: Human; Choroid plexus; Cell line; *in vitro*; *Listeria monocytogenes*; Invasion

1. Introduction

Listeria monocytogenes (*L. monocytogenes*) is a Gram-positive, facultative intracellular bacterium known to cause listeriosis, an infection with a 30% mortality rate in humans. The disease is known to target immunocompromised individuals and is characterized by febrile gastroenteritis, infection of the fetus in pregnant women and central nervous system (CNS) infections, such as meningitis and meningoencephalitis [1,2].

Being a food-borne pathogen, *L. monocytogenes* typically enters the host via the gastrointestinal tract, where it can cross the intestinal epithelium. After dissemination via the lymph and blood stream, *L. monocytogenes* resides in the liver and

* Corresponding author. Tel.: +49 621 383 1299; fax: +49 621 383 3818.
E-mail address: christian.schwerk@medma.uni-heidelberg.de (C. Schwerk).

1286-4579/$ - see front matter © 2013 Institut Pasteur. Published by Elsevier Masson SAS. All rights reserved.
http://dx.doi.org/10.1016/j.micinf.2012.12.005

spleen, where it multiplies and can lead to the formation of abscesses. Once inside the host, the ability of *L. monocytogenes* to breach further epithelial barriers, namely the fetoplacental barrier and the blood–brain barriers, is of special importance [1,3]. The main function of the blood–brain barriers, the maintenance of a metabolic and biochemical homeostasis within the CNS, is upheld by two distinct anatomical structures: first, the "classical" blood–brain barrier (BBB) constituted by cerebral microvascular endothelium in conjunction with pericytes and astrocytes, which separates blood from the brain parenchyma utilizing tight junctions and a lack of pinocytosis, and second, the choroid plexus epithelium, which is the morphological correlate of the blood–cerebrospinal fluid (CSF) barrier (BCSFB). The choroid plexus epithelium is polarized, presents tight junctions and produces CSF. It is situated right above fenestrated capillaries that, unlike the cerebral microvascular endothelium, do not contribute to the function of this particular barrier [4,5].

The crossing of these major barriers by *L. monocytogenes* has long been under scrutiny from researchers and important virulence factors mediating its internalization, escape from the phagosome, intra- and intercellular movement and more, have been identified [6,7]. For entry into non-phagocytic host cells the two surface proteins Internalin (InlA) and InlB are essential [8–10]. Both proteins can bind to receptors located on the surface of host cells, which leads to receptor-mediated internalization of *L. monocytogenes*. InlA binds to the adherens junction protein E-Cadherin (Ecad), whereas InlB interacts with the receptor tyrosine kinase Met, also known as hepatocyte growth factor (HGF) receptor [11,12]. Involvement of co-ligands like CD44v6 during InlB–Met interaction is currently under debate [13,14].

Interestingly, listerial invasion of the intestinal epithelium mainly requires InlA [15,16], although a function of InlB during activation of junctional endocytosis leading to acceleration of intestinal invasion has been described [17]. More recently it was shown that for targeting and crossing of the fetoplacental barrier, both InlA and InlB are required interdependently [18]. So far only few studies have tried to elucidate the role of internalin family proteins during the invasion of the CNS: as suggested by *in vitro* studies, only InlB is thought to mediate invasion in human brain microvascular endothelial cells (HBMEC) [19–22]. This stands in contrast to the detection of Ecad in microvascular epithelium and choroid plexus cells, indicating a possible involvement of InlA [23].

Despite the high incidence of meningitis and meningoencephalitis in humans during infection with *L. monocytogenes*, its pathogenesis and especially the mechanisms involved in breaching the blood brain barriers remain incompletely understood [1,3]. As suggested by *in vivo* studies, *L. monocytogenes* regularly invades the choroid including the plexus epithelial cells and is also found in the CSF following infection [24–26]. Therefore, a route of infection via the BCSFB is worth considering. The lack of information regarding the interaction of *L. monocytogenes* and the choroid plexus epithelium stems from the fact that until very recently, no suitable human model of the choroid plexus had been characterized. In a recent study, our laboratory described a functional human BCSFB *in vitro* model based on human choroid plexus papilloma (HIBCPP) cells [27,28].

Employing the HIBCPP cell-based model, we are now able to demonstrate that *L. monocytogenes* is able to invade HIBCPP cells in a polar fashion from the physiologically relevant basolateral side ("blood-side") only. In strong contrast, *L. monocytogenes* accessing HIBCPP cells from the apical cell membrane ("CSF-side") is rarely found inside the cytosol. Importantly, receptors involved in bacterial entry (i.e. E-Cadherin, Met) are largely absent from the apical membrane in HIBCPP cells. Furthermore, we find the polar entry of *L. monocytogenes* into HIBCPP cells to be strongly dependent on both InlA and InlB, since invasion of HIBCPP cells by isogenic mutant strains lacking either one of these two surface proteins is strongly attenuated. The invasion levels of *L. monocytogenes* lacking either InlA or InlB are comparable to that of a mutant lacking both proteins of the internalin family.

2. Material and methods

2.1. Bacterial strains and growth conditions

L. monocytogenes EGD and its isogenic mutant strains EGDΔInlA, EGDΔInlB, EGDΔInlAB have been described previously [8,29,30]. The identity of the bacterial strains was confirmed by polymerase chain reaction (PCR) and the expression patterns of the genes encoding for InlA and InlB in *L. monocytogenes* EGD and the mutant strains were verified by reverse transcribed PCR (RT-PCR). All strains were maintained as stock cultures in brain–heart infusion (BHI) containing 10% glycerol at −80 °C. For our experiments 100 µl of bacteria stocks were inoculated in 10 ml BHI and incubated at 37 °C for about 6 h with mild agitation to mid-log phase. *L. monocytogenes* cultures were washed twice with serum-free medium (SFM) without antibiotics and then adjusted to an optical density at 600 nm (OD_{600}) of 0.65. These stock solutions had approximately 3×10^8 colony-forming units (CFU) ml^{-1} (EGD wild type, EGDΔInlA, EGDΔInlAB) or 6×10^8 CFU ml^{-1} (EGDΔInlB), respectively, and were further diluted in fresh HIBCPP cell-medium (DMEM/HAM's F12 1:1 supplemented with 4 mM L-glutamine and 5 µg ml^{-1} insulin) without antibiotics containing 1% heat inactivated fetal calf serum (FCS) for the experiments.

2.2. Cultivation of HIBCPP cells on cell culture inserts and measurement of TEER

HIBCPP cells were cultured in DMEM/HAM's F12 1:1 supplemented with 4 mM L-glutamine, 5 µg ml^{-1} insulin, penicillin (100 U ml^{-1}) and streptomycin (100 µg ml^{-1}) (HIBCPP cell-medium) containing 15% heat inactivated fetal calf serum (FCS) and grown in the standard as well as in the inverted cell culture insert system essentially as previously described [27]. Only cells between passage 32 and 38 were used.

HIBCPP had a seeding density of approximately 1.2×10^6 cells cm^{-2} upon confluence as determined by 4,6-diamidino-

2-phenylindole staining of the cell nuclei using immunofluorescence imaging. The transepithelial electrical resistance (TEER) of HIBCPP cells grown on the cell culture inserts was measured with an epithelial tissue voltohmmeter employing the STX-2 electrode system (Millipore, Schwalbach, Germany). Cell culture was switched to HIBCPP-medium containing 1% FCS and no antibiotics, when the TEER became greater than 70 $\Omega \times cm^2$.

2.3. Infection of HIBCPP cells with L. monocytogenes

For infection experiments the multiplicity of infection (MOI) of the *L. monocytogenes* strains was calculated based on the number of cells per well at confluence (1.2×10^6 cells cm^{-2}). HIBCPP cells with a TEER between 400 $\Omega \times cm^2$ and 800 $\Omega \times cm^2$ were exposed to bacteria with an MOI of 10 in HIBCPP cell-medium without antibiotics and containing 1% FCS from the upper compartment of the cell culture insert. This experimental setting enables us to infect HIBCPP cells from the apical side in the standard cell culture insert system and from the basolateral side in the inverted cell culture insert system. Subsequent to infection, TEER across the cell layers was monitored for 4 h. The resistance values of cells on cell culture inserts in the absence of bacteria were measured as control values.

2.4. Determination of paracellular permeability

Paracellular permeability of HIBCPP cell monolayers was determined by monitoring the passage of an FITC-inulin (a small polysaccharide with an average molecular weight of 3000–6000; Sigma, Deisenhofen, Germany) tracer solution (100 μg ml^{-1}) from the apical to the basolateral compartment of cell culture inserts using a Tecan Infinite M200 Multiwell reader (Tecan, Switzerland) over a range of up to 4 h post-infection as previously described [27,31].

2.5. Immunoblot

For detection of Hsp60 whole protein was extracted from HIBCPP cells with modified RIPA buffer (50 mM Tris–HCl (pH 8.0), 2 mM EDTA, 150 mM NaCl, 0.1% SDS, 1% Triton X-100, 1% sodium deoxycholate, 50 mM NaF, 1 mM Na_3VO_4, 1 mM PMSF, protease inhibitor cocktail). 20 μg of protein samples were separated on 4–12% NuPAGE Bis–Tris gels (Invitrogen, Karlsruhe, Germany) and electrophoretically transferred onto nitrocellulose membranes. Protein detection was performed with appropriate primary (rabbit–anti-Hsp60 (Abcam, Cambridge, UK; 1:10,000 diluted), mouse–anti-β-actin (Sigma, Deisenhofen, Germany; 1:10,000 diluted)) and secondary (HRP-conjugated donkey–anti-rabbit or donkey–anti-mouse (Millipore, Schwalbach, Germany; each diluted 1:5000)) antibodies. Protein-staining was visualized using the Immobilon Western Kit (Millipore, Schwalbach, Germany).

For detection of CD44v6, cells were lysed in SDS sample buffer containing 100 mM dithiothreitol (DTT), boiled and subjected to western blot analysis using the human anti-CD44v6 antibody (VFF18), a gift from Bender (Vienna, Austria).

2.6. Immunohistochemistry

Immunohistochemistry was performed as described [27]. The following primary antibodies were used: mouse–anti-E-Cadherin (BD, Heidelberg, Germany; 1:100 diluted), goat–anti-Met (Abcam, Cambridge, United Kingdom; 1:50 diluted), rabbit–anti-ZO1 (Zymed, San Francisco, CA; 1:250 diluted). As secondary antibodies 1:250 dilutions of a donkey–anti-mouse Alexa Flour 594, a donkey–anti-goat Alexa Fluor 594 or a chicken–anti-rabbit Alexa Fluor 594, respectively, were used (all from Molecular Probes, Oregon, USA).

2.7. Determination of bacterial invasion by double immunofluorescence

This was done as previously described [32] with some modifications [27]. *L. monocytogenes* strains were used to infect HIBCPP cells grown on cell culture inserts. Bacteria were detected with a primary antibody against *L. monocytogenes* (rabbit–anti-*L. monocytogenes*; Meridian Life Science, Memphis, TN; 1:500 diluted) and the following secondary antibodies: Alexa Fluor 594 (red) chicken–anti-rabbit antibody (1:250; Molecular Probes, Oregon, USA) or Alexa Fluor 488 (green) donkey–anti-rabbit antibody (1:500; Molecular Probes, Oregon, USA) to stain intra- and extracellular bacteria, respectively. The actin cytoskeleton and the cell nuclei were stained with Phalloidin Alexa Fluor 660 (1:250; Molecular Probes, Oregon, USA) and 4′-6-diamidino-2-phenylindole dihydrochloride (DAPI) (1:50,000), respectively. Assays were performed at least in triplicates for each value and were repeated at least three times. Pictures were scanned and then processed using Adobe Photoshop.

2.8. Electron microscopy

For transmission electron microscopic analyses HIBCPP cells were grown in the inverted cell culture insert system and exposed to bacteria (MOI of 10) for 4 h as described above. Filters were washed once with SFM and fixed for at least 4 h in a 2% glutaraldehyde solution in 75 mM cacodylate buffer (pH 7.4). Filters were washed twice with 75 mM cacodylate buffer (pH 7.4) followed by removal of the support films from the wells with a sharp ophthalmic scalpel. The filters were then cut into stripes, fixed in 1% osmium tetroxide (OsO_4) in cacodylate buffer for 1 h and dehydrated in ascending series of ethanol and propyleneoxide. Contrast enhancement was done by bloc-staining in uranyl-acetate in 70% ethanol for 4 h and flat-embedding in Araldite (Serva, Heidelberg, Germany). Semi-(1 μm) and ultrathin sections (50 nm) were cut using an ultramicrotome (Ultracut R, Leica, Bensheim, Germany). Ultrathin sections were stained with lead citrate followed by mounting on copper grids and final analysis with a Zeiss EM10 (Oberkochen, Germany) electron microscope.

2.9. Measurement of cell viability

Vitality of HIBCPP cells was measured using a Live/Dead assay (Invitrogen, Karlsruhe, Germany) following the instructions of the manufacturer. Fluorescence microscopic pictures were taken to document the results.

2.10. Statistical analysis

Statistical analysis was done using Student's *t*-test after testing for differences of variances. *P*-values were considered significant, highly significant or extremely significant when <0.05, <0.01 or <0.001, respectively. Data represent means + standard deviation (SD).

3. Results

3.1. HIBCPP cells express surface receptors required for listerial adhesion and invasion

We previously established "standard" and "inverted" cell culture insert systems of porcine and human models of the BCSFB, which allow infection of choroid plexus epithelial cells from the apical ("CSF") or the basolateral ("blood") side, respectively [27,31]. HIBCPP cells grown in the inverted cell culture insert system were analyzed for the expression of receptors known to be involved during invasion of *L. monocytogenes* into host cells. Immunofluorescence analysis demonstrated the expression of the main receptors for InlA and InlB (Fig. 1A–D), Ecad and Met, respectively [11,12]. Importantly, both Ecad (Fig. 1A and B) and Met (Fig. 1C and D) are localized exclusively on the basolateral side of HIBCPP cells. Apotome immunofluorescence imaging clearly shows that in HIBCPP cells nearly no staining can be detected for either Ecad or Met at the cell membrane apically to the signal of the tight junction marker ZO1 (Fig. 1B and D). In contrast, staining of the actin cytoskeleton demonstrates a clear signal at the apical side of HIBCPP cells (Fig. 1A and C). CD44v6 and heat shock protein 60 (Hsp60) have been described as co-receptor during InlB–Met mediated invasion of *L. monocytogenes* [14] or as receptor for the 104 kDa *Listeria* adhesion protein (LAP) [33], respectively. Western blot analysis of HIBCPP cells revealed expression of both CD44v6 (Fig. 2E) and Hsp60 (Fig. 2F).

3.2. HIBCPP cells maintain their barrier function during infection assays using L. monocytogenes

To investigate listerial invasion of HIBCPP cells, we infected epithelial layers cultivated in the standard as well as the inverted cell culture insert system with the *L. monocytogenes* wild type strain EGD and isogenic mutant strains lacking either InlA (EGDΔInlA), InlB (EGDΔInlB), or both surface proteins (EGDΔInlAB) at a multiplicity of infection (MOI) of 10 for 2 h and 4 h, respectively. 0 h, 2 h and 4 h post-infection the transepithelial membrane potential was recorded by determining the transepithelial electric resistance (TEER) (Fig. 2A). The TEER did not change after 2 h for the inverted cell system, but decreased slightly for strains EGD and EGDΔInlA at 4 h. Notably, the measured TEER for the standard cell culture insert system decreased significantly to about 300 $\Omega \times cm^2$ at the 4 h time-point with all *L. monocytogenes* strains (Fig. 2A). Live/Dead assays were performed to control cell viability for all experimental conditions. Compared to the significant decrease in TEER after 4 h in the standard cell culture, cell viability was essentially unaffected. No effect on cell viability was seen in the inverted cell culture system (data not shown).

Increasing TEER is associated with an increased impermeability of the cell layer for macromolecules. During each experiment we determined the flux of FITC-labeled inulin. Our results show that infection with the different *L. monocytogenes* strains did not lead to a permeability increase for inulin in the standard as well as the inverted cell culture insert system (Fig. 2B). Despite the described decrease in TEER after 4 h in the standard cell culture insert system, the impermeability of the barrier for FITC-labeled inulin was not affected under these conditions as well.

3.3. Polar invasion of L. monocytogenes into HIBCPP cell layers

Taking into account the polarized nature of the choroid plexus epithelium and previous experiments demonstrating the polar invasion of *Streptococcus suis* and *Neisseria meningitidis* into HIBCPP cell and PCPEC layers [27,31], we considered a similar way of entry for *L. monocytogenes.* To confirm this hypothesis, HIBCPP cells grown in the standard and inverted cell culture insert system were infected for 2 h and 4 h with wild type *L. monocytogenes* EGD at an MOI of 10. Invasion rates were analyzed by double immunofluorescence assays as described in Material and methods.

As can be seen in Fig. 3, we observed significantly ($p < 0.01$) higher invasion rates for bacteria applied in the inverted culture system compared to the standard system after 2 h as well as 4 h of infection. Intracellular *L. monocytogenes* specimens were rarely detected in the standard cell culture insert system. After 2 h of infection, invasion from the basolateral side was 0.006% in the standard cell culture insert system and 0.052% in the inverted cell culture insert system (8.7-fold difference). After 4 h of infection, listerial invasion was 0.005% in the standard cell culture insert system and 0.412% in the inverted cell culture insert system (82.4-fold difference). Taken together, our data strongly suggest a polar route of invasion of *L. monocytogenes* wild type strain EGD from the basolateral side of the HIBCPP cell epithelial layer.

3.4. InlA and InlB are interdependently required for the invasion of HIBCPP cells

The listerial surface proteins InlA and InlB are critical for the invasion of various host cells [34,35]. To establish the role of these virulence factors during the invasion of the CNS via

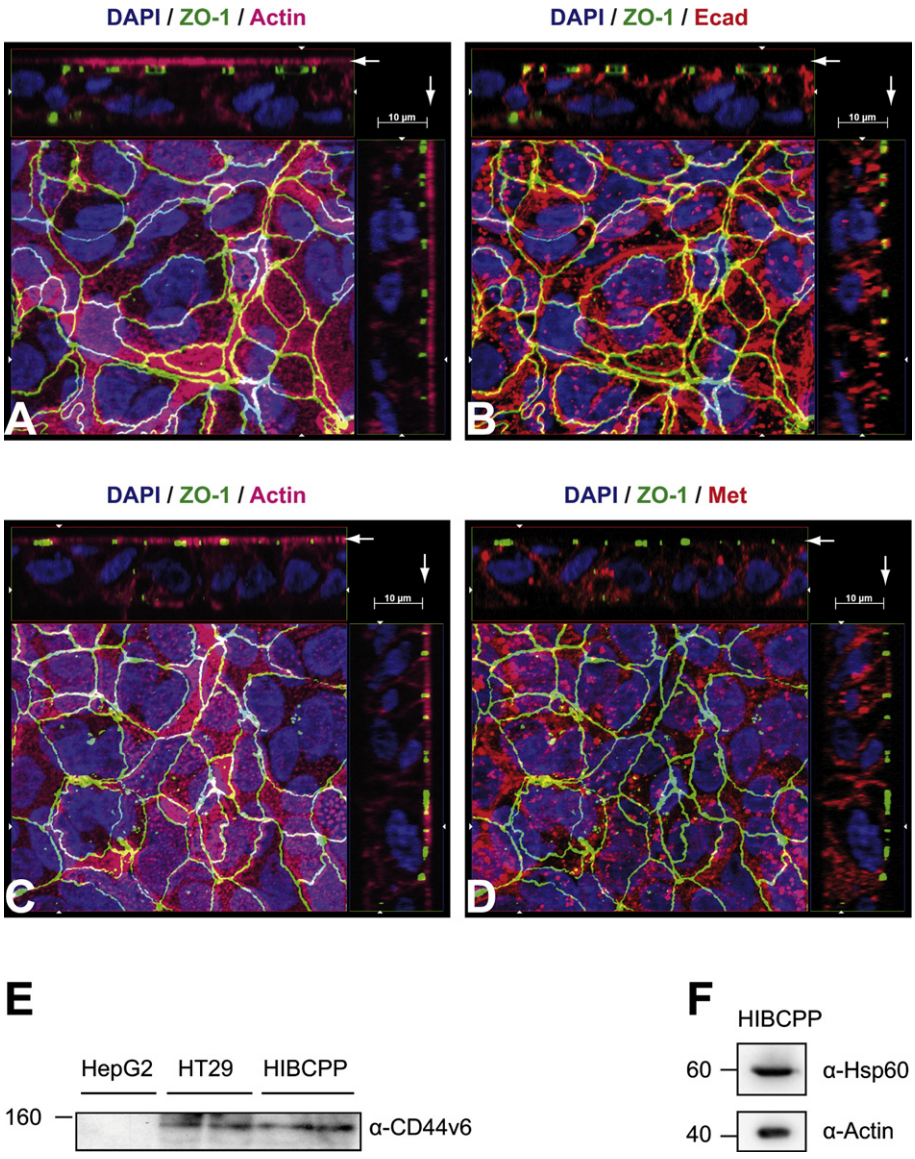

Fig. 1. HIBCPP cells express proteins involved during adhesion and invasion of host cells by *L. monocytogenes*. Expression of E-Cadherin (Ecad) (A, B) and Met (C, D) in HIBCPP cells grown in the inverted filter system are analyzed by immunofluorescence microscopy. Staining of Ecad (B) and Met (D) are shown in red, the actin cytoskeleton was visualized with phalloidin (A, C; magenta). Cell nuclei were stained with 4,6-diamidino-2-phenylindole (blue). Tight junctions were detected with an antibody against ZO1 (green). Panels A–D represent Apotome images. The center part of each panel shows an *xy* en face view of infected HIBCPP cells. Presented is a maximum-intensity projection through the *z*-axis of selected slice. The top and right side part of each panel are cross-sections through the *z*-plane of multiple optical slices. The apical side of HIBCPP cells (indicated by arrows) is oriented towards the top of the top part and towards the right of the right side, respectively, of each panel. Ecad and Met staining is absent from the apical membrane of HIBCPP cells. Expression of CD44v6 (E) and Hsp60 (F) in whole cell extract from HIBCPP cells was detected by immunoblotting. Analysis of extracts from HepG2 and HT29 cells (E) served as negative and positive control, respectively. Two samples were loaded for each cell line. Size markers for apparent molecular weight are indicated. (For interpretation of the references to colour in this figure legend, the reader is referred to the web version of this article.)

the BCSFB we infected HIBCPP cells with three isogenic mutant strains, lacking InlA (EGDΔInlA), InlB (EGDΔInlB), or both surface proteins (EGDΔInlAB), respectively. After 2 and 4 h, respectively, the total numbers of the three mutant strains inside of the cells was quantified by double immunofluorescence assays.

As shown in Fig. 3, the number of intracellular bacteria inside HIBCPP cells increased during the time period studied in the inverted cell culture insert system. It is of interest to note that, like the wild type strain, the three mutant strains invaded HIBCPP cells polarly from the basolateral side. A significantly higher invasion from the basolateral side was observed for strain EGDΔInlA 2 h ($p < 0.05$) and 4 h ($p < 0.01$) post-infection. However, the strains EGDΔInlB and EGDΔInlAB displayed a significantly higher invasion from the basolateral side only 4 h post-infection ($p < 0.01$ for EGDΔInlA and EGDΔInlB, $p < 0.05$ for EGDΔInlAB).

All three mutant strains exhibited similarly low mean relative invasion rates compared to the higher invasion rates of the wild type strain EGD. After 2 h all three mutants entered

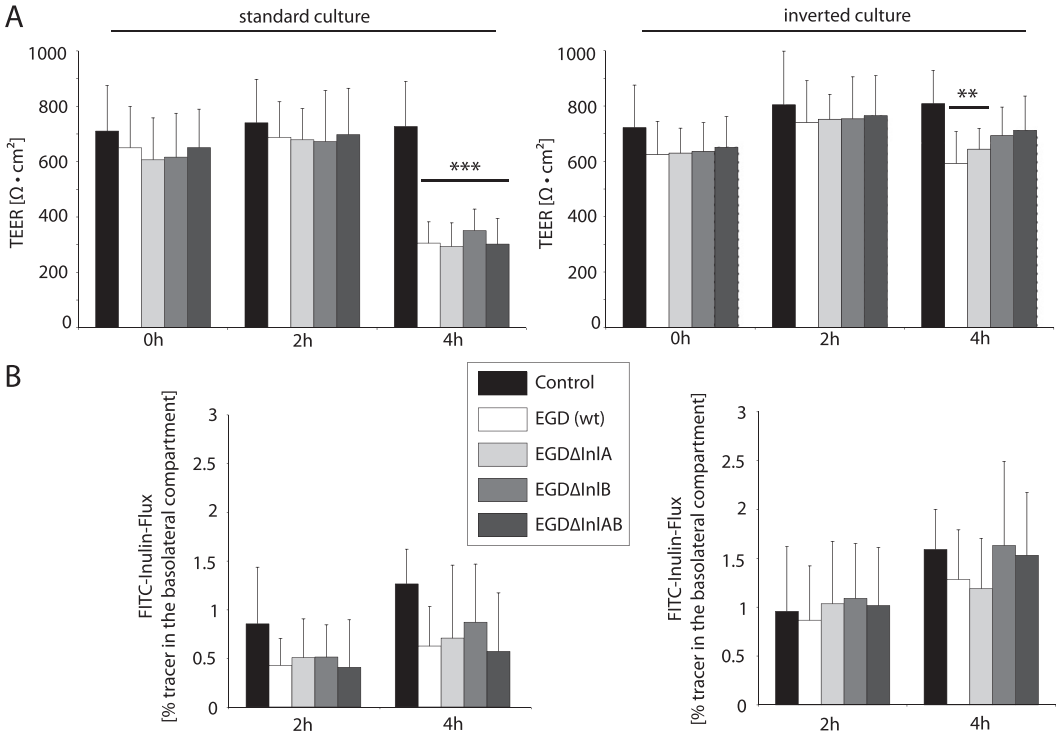

Fig. 2. Apical and basolateral infection of HIBCPP cells with *L. monocytogenes* does not affect barrier function. *L. monocytogenes* wild type (wt) EGD and mutant strains EGDΔInlA, EGDΔInlB and EGDΔInlAB were applied at an MOI of 10 to HIBCPP cell layers grown in the standard (left panels) and inverted (right panels) cell culture insert system and barrier function was determined at the indicated time-points. Effects on barrier function were measured by TEER (A) and FITC-inulin flux (B) of HIBCPP cell layers. The FITC-inulin flux was measured in apical-to-basolateral direction and is expressed as percentage of tracer in the basolateral compartment. Also shown are values for uninfected control filters. Data shown are mean + SD of a minimum of four independent experiments each performed at least in triplicates. ** highly significant, $p < 0.01$, *** extremely significant, $p < 0.001$; when TEER after infection with a mutant strain was compared to the wild type at the same time-point.

HIBCPP cells significantly ($p < 0.05$) less, with the mean invasion rate of the three mutants reduced about 12.1-fold in comparison to the wild type. After 4 h of infection the invasion rates of all mutants were again significantly ($p < 0.01$) reduced compared to that of the wild type strain, with an about 4.3-fold difference. Interestingly, when comparing the invasion rates of the single mutants (i.e. EGDΔInlA and EGDΔInlB) with that of the double mutant EGDΔInlAB no differences were observed, except for EGDΔInlA at the 2 h time-point ($p < 0.05$).

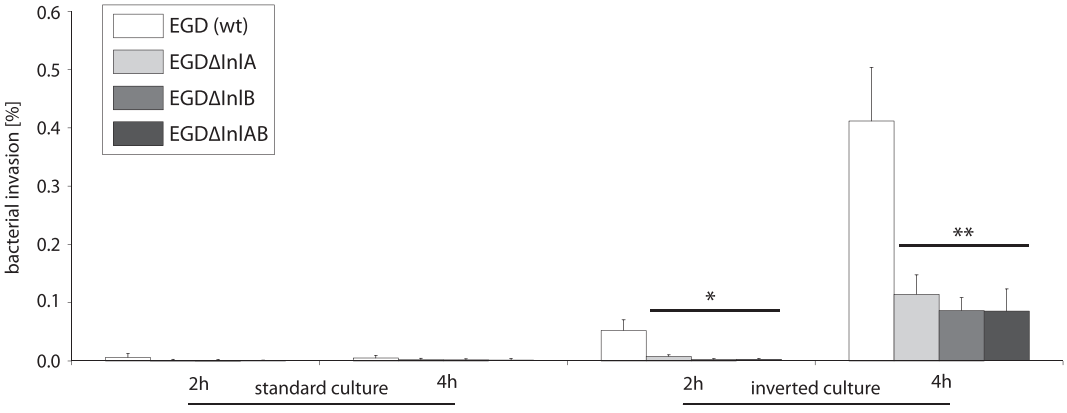

Fig. 3. Polar invasion of *L. monocytogenes* into HIBCPP cells is dependent on proteins of the internalin family. Invasion of *L. monocytogenes* strains was analyzed by double immunofluorescence. Standard and inverted insert cultures were infected with the indicated strains for 2 h and 4 h, respectively, before immunofluorescence staining and quantification of invasion as described in Material and methods. Data shown are mean + SD of a minimum of three independent experiments each performed at least in triplicates. * significant, $p < 0.05$, ** highly significant, $p < 0.01$; when invasion of a mutant strain was compared to that of the wild type in the same culture at the same time-point.

3.5. Intracellular listeria are found in vacuoles and the cytoplasm, where they are often associated with "actin tail"-like structures

Apotome immunofluorescence images of HIBCPP cells after infection with *L. monocytogenes* showed that all strains employed in this study adhered (yellow stained bacteria) regularly to the apical surface of HIBCPP cells in the standard cell culture insert system at both 2 h and 4 h (Fig. 4A–D and Supplementary Fig. S1). Notably, after 4 h of infection clusters of adhered bacteria were occasionally found on the apical surface for all four *L. monocytogenes* strains. Examples are shown for the wild type EGD (Fig. 4A and B) and for EGD-ΔInlAB (Fig. 4C and D). Occasionally, the clusters were accompanied by minor cell destruction at these sites, rarely allowing bacteria to enter into adjoining cells (Fig. 4C; arrow). However, mean invasion rates were still extremely low overall (Fig. 3).

To analyze invasion of *L. monocytogenes* from the basolateral side, we analyzed Apotome immunofluorescence images from HIBCPP cells grown in the inverted cell culture insert system after 2 h and 4 h of infection. In contrast to the standard culture system, we readily detected intracellular bacteria for all four strains, increasing with time (Fig. 4E–H and Supplementary Fig. S2). Interestingly, intracellular *L. monocytogenes* specimens were generally closely associated to actin fibers or clumps of actin. Aggregation of actin around bacteria of all four strains was particularly obvious after 4 h of infection and sometimes appears to form tail-like structures, reminiscent of previously described "actin comet tails" [36,37]. Examples are shown for the wild type EGD (Fig. 4E and F) and for EGDΔInlAB (Fig. 4G and H). *L. monocytogenes* is known to move intra- and intercellularly by hijacking the host cell actin machinery via the use of virulence factor ActA [38].

Electron microscopic images were obtained to substantiate the findings made by immunofluorescence microscopy and to gain additional information concerning the intracellular life of *L. monocytogenes* inside HIBCPP cells (Fig. 5). We examined inverted culture samples that were infected for 4 h, as we barely detected any intracellular bacteria in the standard cell culture insert system. Most importantly, intracellular bacteria were detected for all four strains, particularly many in cells infected with *L. monocytogenes* wild type, confirming our previous analyses. Bacteria were often found free in the cytosol (right and left bacteria in Fig. 5B), whereas some were surrounded by single membranes (Fig. 5B, arrow). Wild type bacteria were mainly localized basally but also at different heights throughout the epithelial cells. In contrast, mutant bacteria were only observed near the basolateral membrane. EGDΔInlAB bacteria were not observed to have moved above cell culture insert filter level. We never observed bacteria between cells. As assumed after the immunofluorescence analysis, high density of actin fibers was detected around single bacteria (Fig. 5C, D, G and H). At times these fibers seemed well organized (Fig. 5D), akin to the morphology of actin comet tails [36,37].

4. Discussion

The crossing of the host blood–brain barriers is a crucial act of any pathogen invading the brain to cause meningitis [39,40]. Discussed mechanisms for CNS invasion by *L. monocytogenes* are a "trojan-horse"-like transport inside of infected monocytes [1,41,42], centripetal migration of bacteria within peripheral axons into the brainstem via a neural route [1], and internalin family protein-mediated invasion of cellular barriers constituting the "classical" BBB [19–22] or the BCSFB [23]. Whereas the impact of InlA and InlB during the internalization process of *L. monocytogenes* has been investigated before for several other cell types [35], no viable *in vitro* model for the choroid plexus epithelium existed, making analysis of the human BCSFB difficult. In particular, the interaction of InlA with its receptor Ecad is not functional in rats and mice, and Met does not function as a receptor for InlB in guinea pigs. Although the gerbil is a small animal permissive to both InlA and InlB, a human model for analysis of invasion by *L. monocytogenes* is of special interest [34]. Elucidation of the InlA–Ecad interaction at the BCSFB seems particularly interesting when taking into account the potential accessibility of Ecad at the basolateral cell membrane of the choroid plexus epithelium from the blood [23].

Here we made use of the human choroid plexus papilloma epithelial cell line HIBCPP grown in an inverted cell culture insert system, which allows analysis of bacterial invasion from the physiological relevant basolateral side [27,31]. We found that HIBCPP cells expressed Ecad, Met, CD44v6 and Hsp60. Presumably, Hsp60 can mediate paracellular transmigration through epithelial cell layers via interaction with the adhesion protein LAP of *L. monocytogenes* [33,43]. Although we did not find bacteria located between HIBCPP cells in our infection experiments, we cannot decisively exclude paracellular crossing of HIBCPP cell layers by some listeria. Importantly, Ecad and Met were largely absent from the apical side of HIBCPP cells and almost exclusively localized basolaterally. Basolateral localization of Ecad has also been described for the human choroid plexus epithelium [44]. Therefore, even though to our knowledge no information is available regarding the expression of Met at the human choroid plexus, HIBCPP cells seem, at least partly, to reflect the physiological *in vivo* situation.

The confluence of the cell layer and its impermeability for macromolecules remained intact for up to 4 h of infection. Employing this model we were able to demonstrate invasion of *L. monocytogenes* into HIBCPP cells. Invasion occurred strongly polar from the basolateral side, which can be explained with the polar localization of Ecad and Met at the basolateral membrane of HIBCPP cells. Bacteria were found in vacuoles as well as free in the cytosol, sometimes associated with masses of actin filaments, pointing to the described life style of intracellular *L. monocytogenes* [38]. In the electron microscopic studies the majority of bacteria were found at basal locations, sometimes within the filter pores. This is very likely due to the limited number of bacteria that within the 4 h time-frame moved towards more apical locations, and which

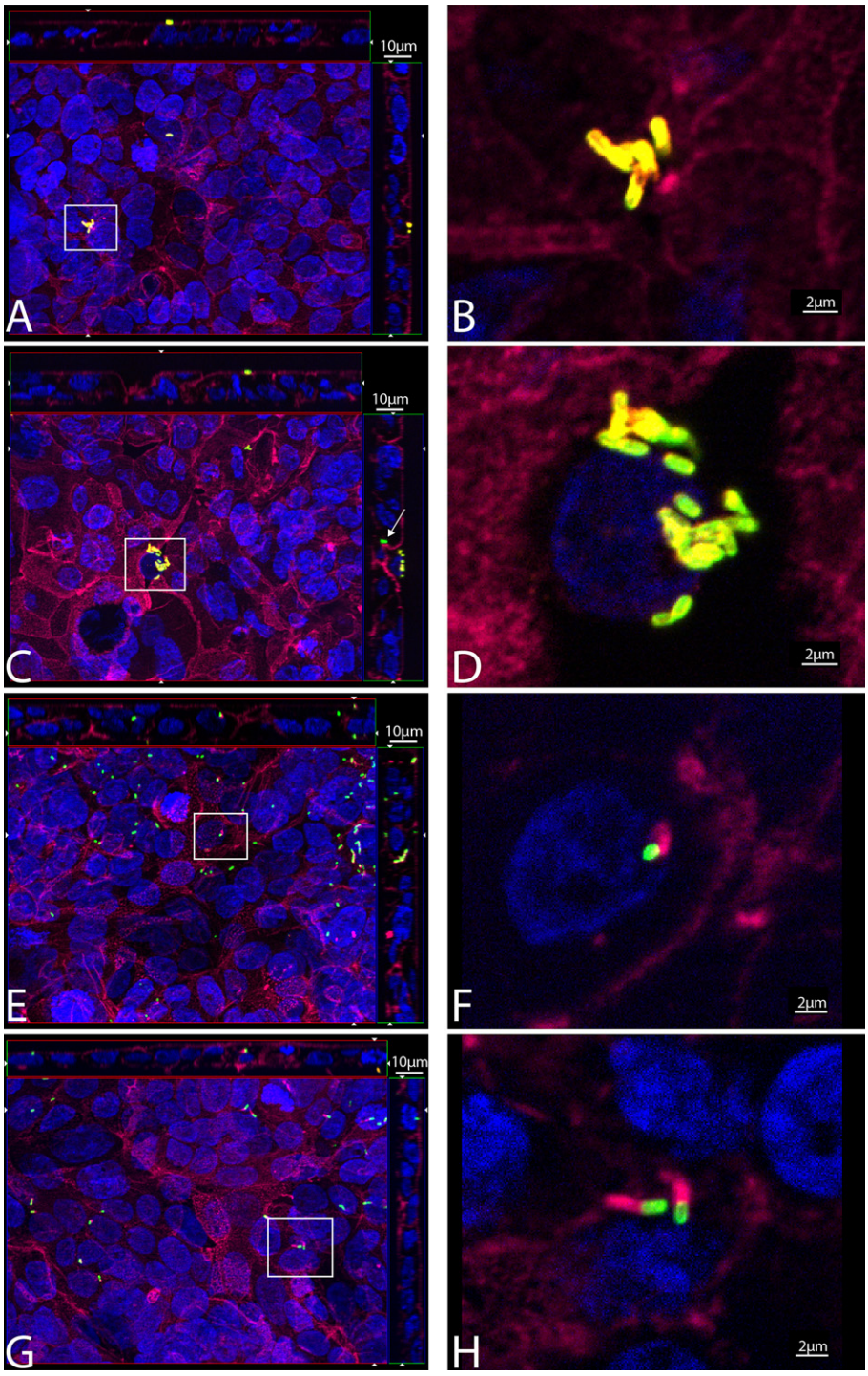

Fig. 4. Double immunofluorescence microscopy of adherence and invasion of HIBCPP cells infected with *L. monocytogenes*. HIBCPP cells were grown in the standard (A–D) or inverted (E–H) cell culture insert system. Cells were challenged (MOI 10) with *L. monocytogenes* wild type EGD (A, B and E, F) or the mutant strain EGDΔInlAB (C, D and G, H) for 4 h, respectively, and subjected to double immunofluorescence microscopy to detect intracellular (green) and extracellular (yellow) bacteria. Cell nuclei were 4,6-diamidino-2-phenylindole (blue)-stained. The actin cytoskeleton was visualized with phalloidin (magenta). Panels A, C, E and G represent Apotome images. The center part of each panel shows an *xy* en face view of infected HIBCPP cells. Presented is a maximum-intensity projection through the *z*-axis of selected slice. The top and right side part of each panel are cross-sections through the *z*-plane of multiple optical slices. The apical side of HIBCPP cells is oriented towards the top of the top part and towards the right of the right side part, respectively, of each panel. Panels B, D, F and H present enlargements of the areas indicated in A, C, E and G, respectively. Wild type *L. monocytogenes* and strain EGDΔInlAB show adherence to the apical membrane, but hardly any invasion (A–D). Note that some clusters of adhered bacteria at the apical membrane could be observed. Few invaded bacteria tended to be located near such bacterial clusters (C; arrow). Wild type *L. monocytogenes* and strain EGDΔInlAB invaded HIBCPP from the basolateral side (E–H). EGDΔInlAB displayed reduced invasion compared to the wild type. Interestingly, bacteria were often found to be associated with distinct actin structures, reminiscent of the formation of "actin comet tails" (F, H). Adhered bacteria at the basolateral membrane side near cell culture insert pores were regularly found. Shown are representative images of a minimum of three independent experiments all performed in triplicates. (For interpretation of the references to colour in this figure legend, the reader is referred to the web version of this article.)

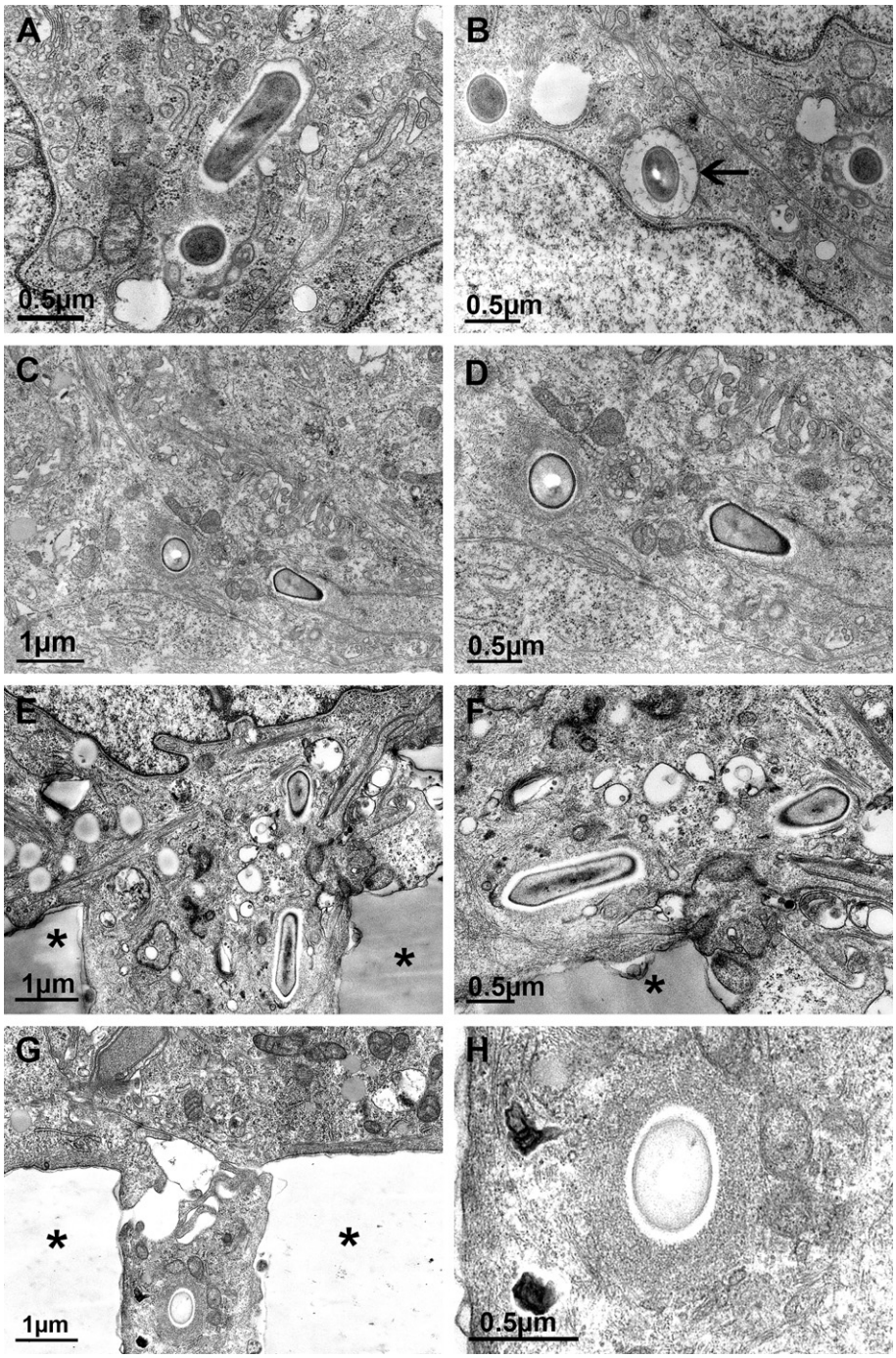

Fig. 5. Electron micrographs of HIBCPP inverted cultures infected with *L. monocytogenes* wild type and mutant strains deficient for proteins of the internalin family for 4 h. A and B show the *L. monocytogenes* wild type strain EGD within epithelial cells. Specimens with intercellular localization could not be observed. Nearly all bacteria were found basally in the cells, not in the apical regions of the cells. Some, but not all bacteria were surrounded by a membrane (arrow in B). C and D show the mutant strain EGDΔInlA in low (C) and higher (D) magnification. Some bacteria were surrounded by masses of actin filaments. E and F show the mutant strain EGDΔInlB in low (E) and higher (F) magnification. These bacteria were found only at an extremely basal localization in the pores of the filter (*). The bacteria were not surrounded by a membrane. G and H show the mutant strain EGDΔInlAB, which could be observed exclusively within the filter pores suggesting either low migration rate or enhanced phagocytosis of the bacteria. H is a detail of G, the specimen is surrounded by actin filaments. (*) filter.

are difficult to spot during electron microscopic analyses. Notably, apically located bacteria could be seen for all employed *L. monocytogenes* strains in immunofluorescence stained samples.

The importance of both InlA and InlB for the direct invasion of the BCSFB *in vitro* could be shown with the help of mutant bacteria lacking either one or both of the internalin family proteins. Clearly, deletion of either InlA or InlB strongly diminished invasion of *L. monocytogenes* into HIBPP, pointing to a role of both surface proteins during cellular entry. After 2 h of infection, the quantitative difference between invaded *L. monocytogenes* wild type and its isogenic mutant

bacteria was particularly striking. After 4 h of infection, this difference was diminished. This decreased difference could possibly be due to saturation effects caused by the very high number of intracellular bacteria at this time-point that might already have been multiplying and spreading inside of the HIBCPP cell layer. It should be noted that deletion of InlA and InlB did not completely abolish entry into HIBCPP cells. This residual capacity is most likely due to the involvement of other listerial factors, including the LPXTG protein Vip and the surface-associated GW repeat-containing protein Auto, which have been described to be involved in cellular invasion [6]. Also, the immunogenic surface protein C of *L. monocytogenes* can contribute to adhesion and invasion of sheep choroid plexus cells [45].

Interestingly, the deletion of both InlA and InlB does not further attenuate invasion compared to the single deletions potentially indicating both to be interdependent. A similar co-dependence of InlA and InlB was also documented for fetoplacental listeriosis *in vivo* [18]. Although the specific mechanisms of this interdependence and the differing roles of InlA and InlB remain unclear, this finding underlines the importance of InlA beyond the intestinal level, which has been questioned before [46]. At the intestinal barrier, InlA promotes the transmigration through the epithelial layer independently of InlB [15,16], although it has been described that InlB functions during activation of junctional endocytosis to accelerate intestinal invasion [17]. In a recent *in vivo* study employing a murine animal model expressing humanized E-Cadherin at the intestinal level, this crossing was shown to be transcytotic and independent of other listerial virulence factors such as Listeriolysin O or ActA [16].

In this manuscript we also described a strictly polar route of invasion of *L. monocytogenes* wild type bacteria into HIBCPP cells from the physiologically relevant basolateral side only. In contrast to challenge of HIBCPP cells with bacteria from the basolateral side in the inverted cell culture insert system, invasion rates were extremely low when *L. monocytogenes* encountered HIBCPP cells from the apical side in the standard cell culture insert system. Interestingly, *L. monocytogenes* invades the polarized human epithelial colorectal adenocarcinoma cell line CaCo-2 predominantly through the basolateral surface [47], and in the intestinal epithelium, Ecad, which is usually located basolaterally of tight junctions in epithelia [48], is frequently exposed at goblet cell–enterocyte junctions and other sites allowing InlA-mediated entry from the apical side [16]. It seems that HIBCPP don't expose Ecad apically as readily, as indicated by the lack of invading listeria expressing InlA. Taking into account our previous results employing *S. suis* and *N. meningitidis* in PCPEC and HIBCPP cells, it is interesting to see that all these bacterial pathogens invade choroid plexus epithelial cells in this polar fashion [27,31], pointing to a more general lack of receptors required for bacterial entry at the apical membrane. These results emphasize the polar nature of HIBCPP cells, which is not easily compromised by bacterial pathogens.

In summary, utilizing *L. monocytogenes* wild type bacteria and isogenic mutant strains to infect human choroid plexus papilloma cells mimicking the BCSFB, we demonstrate internalin family protein-mediated invasion depending on both InlA and InlB for choroid plexus epithelial cells. Furthermore, this invasion occurs in a polar fashion from the *in vivo* relevant basolateral cell side and correlates with the localization of Ecad and Met in HIBCPP cells. The ability of entering the choroid plexus is in concurrence with neuropathological *in vivo* findings of *L. monocytogenes* strongly colonizing the choroid plexus, where they often reside in phagocytotic cells [24–26]. The relevance of direct invasion of free *L. monocytogenes* bacteria into the choroid plexus *in vivo* has not been elucidated so far, which, according to our *in vitro* findings of *L. monocytogenes* specimens readily invading the BCSFB, would be a highly interesting subject for future investigation.

Acknowledgments

The authors would like to thank Dr. Trinad Chakraborty for the *L. monocytogenes* strains. We are grateful for the skillful help in electron microscopy by Gabi Frommer-Kästle.

Appendix A. Supplementary data

Supplementary data related to this article can be found at http://dx.doi.org/10.1016/j.micinf.2012.12.005.

References

[1] D.A. Drevets, M.S. Bronze, Listeria monocytogenes: epidemiology, human disease, and mechanisms of brain invasion, FEMS Immunol. Med. Microbiol. 53 (2008) 151–165.
[2] J.A. Vazquez-Boland, M. Kuhn, P. Berche, T. Chakraborty, G. Dominguez-Bernal, W. Goebel, B. Gonzalez-Zorn, J. Wehland, J. Kreft, Listeria pathogenesis and molecular virulence determinants, Clin. Microbiol. Rev. 14 (2001) 584–640.
[3] F. Stavru, C. Archambaud, P. Cossart, Cell biology and immunology of Listeria monocytogenes infections: novel insights, Immunol. Rev. 240 (2011) 160–184.
[4] N.J. Abbott, A.A. Patabendige, D.E. Dolman, S.R. Yusof, D.J. Begley, Structure and function of the blood–brain barrier, Neurobiol. Dis. 37 (2010) 13–25.
[5] H. Wolburg, W. Paulus, Choroid plexus: biology and pathology, Acta Neuropathol. 119 (2010) 75–88.
[6] A. Camejo, F. Carvalho, O. Reis, E. Leitao, S. Sousa, D. Cabanes, The arsenal of virulence factors deployed by Listeria monocytogenes to promote its cell infection cycle, Virulence 2 (2011) 379–394.
[7] P. Cossart, Illuminating the landscape of host-pathogen interactions with the bacterium Listeria monocytogenes, Proc. Natl. Acad. Sci. U S A 108 (2011) 19484–19491.
[8] S.K. Parida, E. Domann, M. Rohde, S. Muller, A. Darji, T. Hain, J. Wehland, T. Chakraborty, Internalin B is essential for adhesion and mediates the invasion of Listeria monocytogenes into human endothelial cells, Mol. Microbiol. 28 (1998) 81–93.
[9] J.L. Gaillard, P. Berche, C. Frehel, E. Gouin, P. Cossart, Entry of L. monocytogenes into cells is mediated by internalin, a repeat protein reminiscent of surface antigens from gram-positive cocci, Cell 65 (1991) 1127–1141.
[10] S. Dramsi, I. Biswas, E. Maguin, L. Braun, P. Mastroeni, P. Cossart, Entry of Listeria monocytogenes into hepatocytes requires expression of inIB, a surface protein of the internalin multigene family, Mol. Microbiol. 16 (1995) 251–261.

[11] J. Mengaud, H. Ohayon, P. Gounon, R.M. Mege, P. Cossart, E-cadherin is the receptor for internalin, a surface protein required for entry of L. monocytogenes into epithelial cells, Cell 84 (1996) 923–932.
[12] Y. Shen, M. Naujokas, M. Park, K. Ireton, InIB-dependent internalization of Listeria is mediated by the Met receptor tyrosine kinase, Cell 103 (2000) 501–510.
[13] L. Dortet, E. Veiga, M. Bonazzi, P. Cossart, CD44-independent activation of the Met signaling pathway by HGF and InlB, Microbes Infect. 12 (2010) 919–927.
[14] C. Jung, A. Matzke, H.H. Niemann, C. Schwerk, T. Tenenbaum, V. Orian-Rousseau, Involvement of CD44v6 in InlB-dependent Listeria invasion, Mol. Microbiol. 72 (2009) 1196–1207.
[15] M. Lecuit, S. Vandormael-Pournin, J. Lefort, M. Huerre, P. Gounon, C. Dupuy, C. Babinet, P. Cossart, A transgenic model for listeriosis: role of internalin in crossing the intestinal barrier, Science 292 (2001) 1722–1725.
[16] G. Nikitas, C. Deschamps, O. Disson, T. Niault, P. Cossart, M. Lecuit, Transcytosis of Listeria monocytogenes across the intestinal barrier upon specific targeting of goblet cell accessible E-cadherin, J. Exp. Med. 208 (2011) 2263–2277.
[17] M. Pentecost, J. Kumaran, P. Ghosh, M.R. Amieva, Listeria monocytogenes internalin B activates junctional endocytosis to accelerate intestinal invasion, PLoS Pathog. 6 (2010) e1000900.
[18] O. Disson, S. Grayo, E. Huillet, G. Nikitas, F. Langa-Vives, O. Dussurget, M. Ragon, A. Le Monnier, C. Babinet, P. Cossart, M. Lecuit, Conjugated action of two species-specific invasion proteins for fetoplacental listeriosis, Nature 455 (2008) 1114–1118.
[19] L. Greiffenberg, W. Goebel, K.S. Kim, J. Daniels, M. Kuhn, Interaction of Listeria monocytogenes with human brain microvascular endothelial cells: an electron microscopic study, Infect. Immun. 68 (2000) 3275–3279.
[20] L. Greiffenberg, W. Goebel, K.S. Kim, I. Weiglein, A. Bubert, F. Engelbrecht, M. Stins, M. Kuhn, Interaction of Listeria monocytogenes with human brain microvascular endothelial cells: InlB-dependent invasion, long-term intracellular growth, and spread from macrophages to endothelial cells, Infect. Immun. 66 (1998) 5260–5267.
[21] T. Hertzig, M. Weber, L. Greiffenberg, B.S. Holthausen, W. Goebel, K.S. Kim, M. Kuhn, Antibodies present in normal human serum inhibit invasion of human brain microvascular endothelial cells by Listeria monocytogenes, Infect. Immun. 71 (2003) 95–100.
[22] S.L. Wilson, D.A. Drevets, Listeria monocytogenes infection and activation of human brain microvascular endothelial cells, J. Infect. Dis. 178 (1998) 1658–1666.
[23] M. Lecuit, Understanding how Listeria monocytogenes targets and crosses host barriers, Clin. Microbiol. Infect. 11 (2005) 430–436.
[24] P. Berche, Bacteremia is required for invasion of the murine central nervous system by Listeria monocytogenes, Microb. Pathog. 18 (1995) 323–336.
[25] N. Prats, V. Briones, M.M. Blanco, J. Altimira, J.A. Ramos, L. Dominguez, A. Marco, Choroiditis and meningitis in experimental murine infection with Listeria monocytogenes, Eur. J. Clin. Microbiol. Infect. Dis. 11 (1992) 744–747.
[26] D. Schluter, S. Chahoud, H. Lassmann, A. Schumann, H. Hof, M. Deckert-Schluter, Intracerebral targets and immunomodulation of murine Listeria monocytogenes meningoencephalitis, J. Neuropathol. Exp. Neurol. 55 (1996) 14–24.
[27] C. Schwerk, T. Papandreou, D. Schuhmann, L. Nickol, J. Borkowski, U. Steinmann, N. Quednau, C. Stump, C. Weiss, J. Berger, H. Wolburg, H. Claus, U. Vogel, H. Ishikawa, T. Tenenbaum, H. Schroten, Polar invasion and translocation of Neisseria meningitidis and Streptococcus suis in a novel human model of the blood–cerebrospinal fluid barrier, PLoS One 7 (2012) e30069.
[28] I. Ishiwata, C. Ishiwata, E. Ishiwata, Y. Sato, K. Kiguchi, T. Tachibana, H. Hashimoto, H. Ishikawa, Establishment and characterization of a human malignant choroids plexus papilloma cell line (HIBCPP), Hum. Cell 18 (2005) 67–72.
[29] A. Lingnau, E. Domann, M. Hudel, M. Bock, T. Nichterlein, J. Wehland, T. Chakraborty, Expression of the Listeria monocytogenes EGD inlA and inlB genes, whose products mediate bacterial entry into tissue culture cell lines, by PrfA-dependent and -independent mechanisms, Infect. Immun. 63 (1995) 3896–3903.
[30] S.H. Kaufmann, Acquired resistance to facultative intracellular bacteria: relationship between persistence, cross-reactivity at the T-cell level, and capacity to stimulate cellular immunity of different Listeria strains, Infect. Immun. 45 (1984) 234–241.
[31] T. Tenenbaum, T. Papandreou, D. Gellrich, U. Friedrichs, A. Seibt, R. Adam, C. Wewer, H.J. Galla, C. Schwerk, H. Schroten, Polar bacterial invasion and translocation of Streptococcus suis across the blood-cerebrospinal fluid barrier in vitro, Cell. Microbiol. 11 (2009) 323–336.
[32] L. Benga, R. Goethe, M. Rohde, P. Valentin-Weigand, Non-encapsulated strains reveal novel insights in invasion and survival of Streptococcus suis in epithelial cells, Cell. Microbiol. 6 (2004) 867–881.
[33] J.L. Wampler, K.P. Kim, Z. Jaradat, A.K. Bhunia, Heat shock protein 60 acts as a receptor for the Listeria adhesion protein in Caco-2 cells, Infect. Immun. 72 (2004) 931–936.
[34] M. Bonazzi, M. Lecuit, P. Cossart, Listeria monocytogenes internalin and E-cadherin: from structure to pathogenesis, Cell. Microbiol. 11 (2009) 693–702.
[35] K. Ireton, Entry of the bacterial pathogen Listeria monocytogenes into mammalian cells, Cell. Microbiol. 9 (2007) 1365–1375.
[36] L.G. Tilney, D.A. Portnoy, Actin filaments and the growth, movement, and spread of the intracellular bacterial parasite, Listeria monocytogenes, J. Cell Biol. 109 (1989) 1597–1608.
[37] E. Gouin, H. Gantelet, C. Egile, I. Lasa, H. Ohayon, V. Villiers, P. Gounon, P.J. Sansonetti, P. Cossart, A comparative study of the actin-based motilities of the pathogenic bacteria Listeria monocytogenes, Shigella flexneri and Rickettsia conorii, J. Cell Sci. 112 (1999) 1697–1708.
[38] A. Lambrechts, K. Gevaert, P. Cossart, J. Vandekerckhove, M. Van Troys, Listeria comet tails: the actin-based motility machinery at work, Trends Cell Biol. 18 (2008) 220–227.
[39] K.S. Kim, Acute bacterial meningitis in infants and children, Lancet Infect. Dis. 10 (2010) 32–42.
[40] U. Koedel, M. Klein, H.W. Pfister, New understandings on the pathophysiology of bacterial meningitis, Curr. Opin. Infect. Dis. 23 (2010) 217–223.
[41] O.F. Join-Lambert, S. Ezine, A. Le Monnier, F. Jaubert, M. Okabe, P. Berche, S. Kayal, Listeria monocytogenes-infected bone marrow myeloid cells promote bacterial invasion of the central nervous system, Cell. Microbiol. 7 (2005) 167–180.
[42] D.A. Drevets, M.J. Dillon, J.S. Schawang, N. Van Rooijen, J. Ehrchen, C. Sunderkotter, P.J. Leenen, The Ly-6Chigh monocyte subpopulation transports Listeria monocytogenes into the brain during systemic infection of mice, J. Immunol. 172 (2004) 4418–4424.
[43] K.M. Burkholder, A.K. Bhunia, Listeria monocytogenes uses Listeria adhesion protein (LAP) to promote bacterial transepithelial translocation and induces expression of LAP receptor Hsp60, Infect. Immun. 78 (2010) 5062–5073.
[44] D. Figarella-Branger, H. Lepidi, C. Poncet, D. Gambarelli, N. Bianco, G. Rougon, J.F. Pellissier, Differential expression of cell adhesion molecules (CAM), neural CAM and epithelial cadherin in ependymomas and choroid plexus tumors, Acta Neuropathol. 89 (1995) 248–257.
[45] L. Wang, M. Lin, A novel cell wall-anchored peptidoglycan hydrolase (autolysin), IspC, essential for Listeria monocytogenes virulence: genetic and proteomic analysis, Microbiology 154 (2008) 1900–1913.
[46] T. Wollert, B. Pasche, M. Rochon, S. Deppenmeier, J. van den Heuvel, A.D. Gruber, D.W. Heinz, A. Lengeling, W.D. Schubert, Extending the host range of Listeria monocytogenes by rational protein design, Cell 129 (2007) 891–902.
[47] J.L. Gaillard, B.B. Finlay, Effect of cell polarization and differentiation on entry of Listeria monocytogenes into the enterocyte-like Caco-2 cell line, Infect. Immun. 64 (1996) 1299–1308.
[48] C.M. Niessen, Tight junctions/adherens junctions: basic structure and function, J. Invest. Dermatol. 127 (2007) 2525–2532.